

Multi-sensor Data Fusion for Vehicle Detection in Autonomous Vehicle Applications

Abu Hasnat Mohammad Rubaiyat, University of Virginia, Charlottesville, VA 22904-4259

Yaser Fallah; University of Central Florida, Orlando, FL32816-2362, USA

Xin Li; West Virginia University; Morgantown, WV 26506-6109, USA

Gaurav Bansal; Toyota InfoTechnology Center, Mountain View, CA94043.

Abstract

In autonomous vehicle systems, sensing the surrounding environment is important to an intelligent vehicle's making the right decision about the action. Understanding the neighboring environment from sensing data can enable the vehicle to be aware of other moving objects nearby (e.g., vehicles or pedestrians) and therefore avoid collisions. This local situational awareness mostly depends on extracting information from a variety of sensors (e.g. camera, LIDAR, RADAR) each of which has its own operating conditions (e.g., lighting, range, power). One of the open issues in the reconstruction and understanding of the environment of autonomous vehicle is how to fuse locally sensed data to support a specific decision task such as vehicle detection. In this paper, we study the problem of fusing data from camera and LIDAR sensors and propose a novel 6D (RGB+XYZ) data representation to support visual inference. This work extends previous Position and Intensity-included Histogram of Oriented Gradient (PIHOG or π HOG) from color space to the proposed 6D space, which targets at achieving more reliable vehicle detection than single-sensor approach. Our experimental result have validated the effectiveness of the proposed multi-sensor data fusion approach - i.e., it achieves the detection accuracy of 73% on the challenging KITTI dataset.

Introduction

Each year tens of thousands of drivers and passengers lose their lives in the United States due to car accidents. For many years, researchers have been trying to develop a fully automated transportation system for the purpose of reducing on-road fatalities and saving lives. An autonomous vehicle system (AVS) is a combination of several automated systems where perception, decision making, and operation of the automobile are performed by electronics and machinery instead of human drivers. This system includes the control of vehicle movements, destination, path planning, awareness of vehicle environment, inter-vehicle communication, emergency awareness and so on. Successful reconstruction and understanding of the surrounding environment are important to the awareness and safety of AVS; since most fatal crashes involve more than one vehicle, detecting vehicles is one of the most critical issues to the development of AVS. Accordingly, several sensor technologies have been developed to facilitate the task of vehicle detection. In this paper, we focus on a multi-sensor fusion study of improving the performance of vehicle detection by AVS.

For the purpose of vehicle environment reconstruction, automated vehicles use a variety of sensing modalities such as radar,

LIDAR, and camera. As the imaging technology has rapidly progressed in recent years, cameras are widely used in AVS due to their small size, low price, and wide availability. By contrast, LIDAR or point cloud data are relatively newer but a valuable addition to the AVS especially in adversary environments (e.g., nighttime or bad weather). The working principle of LIDAR is to illuminate a target with a pulsed laser light, and then measure the reflected pulses with the LIDAR sensor (e.g. Velodyne HDL) that gives the measurement of the distance from the sensor to the target. Differences in laser return times are used to make digital 3D-representations of the target, which contains XYZ information of the points on that target. Analysis of LIDAR data in AVS has just gained popularity because LIDAR admits computationally more efficient processing and enjoys less vulnerability to adversary weather and lighting conditions comparing with conventional image data. Many researchers have used the data from these two sensors both separately [1][2][3][4][5][6][10] and jointly [7][8][9] in different AVS applications. In this work, we will present an approach of vehicle environment reconstruction based on the fusion of camera and LIDAR data to support the task of vehicle detection from multi-sensor data.

Several researchers have been worked on vehicle detection from image and 3D point cloud data [11]. Kim et al. [12] proposed a Position and Intensity- included Histogram of Oriented Gradients (PIHOG) based vehicle detection approach from color images; Erbs et al. [13] analyzed stixel dynamics to detect moving vehicles from color images. Since achieving scale invariant has been a challenging issue in vehicle detection from color images, some researchers have explored the approach of using 3D point cloud data for resolving this issue. Li et al. [14] used fully convolutional network to detect vehicle from 3D data; Eum et al. [15] presented a novel method for vehicle detection from airborne LIDAR point clouds based on a decision tree algorithm with horizontal and vertical features of the segment. Still, depending on point cloud only (without any color information) is challenging mainly due to the limited resolution and noise interference with point cloud data. In the open literature, the idea of jointly using information from both camera and LIDAR data for detecting vehicle has been scarce (with the exception of [9]). In this paper, we propose to create a novel 6D feature representation of vehicle environment from LIDAR data and RGB image and demonstrate its capability for enhancing the performance of vehicle detection. More specifically, a PIHOG based approach has been applied to the constructed 6D map and a support vector machine (SVM) [18] is used to train the extracted PIHOG features for detecting vehicles on the road. Data sets from the KITTI database [16] have

been used in our experiments and encouraging preliminary results are presented in experimental results section.

Proposed Method

The proposed method of vehicle detection can be described in two steps: 1) Reconstruction of the vehicle environment using LIDAR point cloud data and RGB images from camera; 2) Exploit a PIHOG based approach to detect vehicle from the reconstructed environment.

Analysis of Multi-Sensor Data

Different local sensors (e.g. camera, RADAR, LIDAR etc.) mounted on autonomous vehicles, gather information that can be helpful to understand the surrounding environment of the vehicle. In our proposed method, data from camera and LIDAR are used to reconstruct this so-called vehicle environment. Color images of the roads and other objects are captured using vehicle camera; LIDAR sensor continuously collects a collection of point cloud data surrounding (360 degree) the host vehicle. Each of these point cloud data carries partial information about the environment. Hence, it is desirable to develop a method that can collectively combine multiple point clouds into a whole set. An EM-ICP based multiple point cloud mosaicing technique has been proposed in [10] where a map of the environment is generated from point cloud data containing only the XYZ positions of an object (refer to Figure 1). To obtain a more comprehensive environment representation, we need the color(RGB) image of that object (refer to Figure 2). Therefore, a technique capable of combining point cloud data with color images can provide a better representation of the neighboring environment of the host vehicle. In this work, we propose to fuse the data from these two sensors to generate a six-dimensional representation of the environment that can provide both the XYZ position and RGB color values of any point on the object of interest.

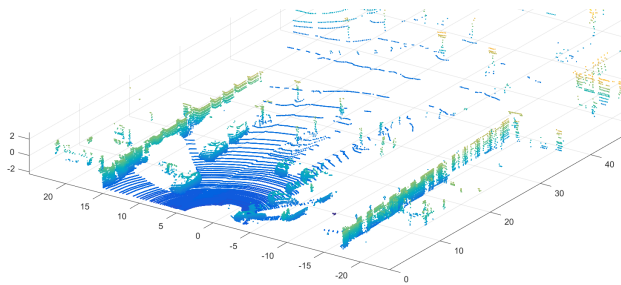


Figure 1: 3D point cloud representation of a scenario



Figure 2: RGB image of the scenario shown in Figure 1

Fusion of Multi-sensor Data

How to fuse the LIDAR data and color image automatically? The key challenge lies in the registration or calibration of these

two types of data (acquired by two sensors with varying physical locations). This problem has been studied in the literature (e.g., [19] where a planar surface of various poses is required). For KITTI data used in our experiment, we have adopted the calibration procedure as described in [16]. A 3D point x in the velodyne coordinates can be projected to a point y in the imaging plane of the i^{th} camera using the following equation

$$y = P_{rect}^i R_{rect}^i T_{velo}^{cam} x; P_{rect}^i \in R^{3 \times 4}, R_{rect}^i \in R^{3 \times 3} \quad (1)$$

where, R_{rect}^i and P_{rect}^i are the rectifying rotation matrix of the i^{th} camera and projection matrix after rectification respectively. Here, $i \in \{0, 1, 2, 3\}$ is the camera index: 0 is for left grayscale, 1 for the right grayscale, 2 the left color, and 3 the right color. Note that only the left color image $i = 2$ has been used in our experiment. T_{velo}^{cam} is the velodyne to camera transformation matrix which is calculated using the following equation

$$T_{velo}^{cam} = \begin{bmatrix} R_{rect}^i & t_{velo}^{cam} \\ 0 & 1 \end{bmatrix} \quad (2)$$

- $R_{velo}^{cam} \in R^{3 \times 3}$ is the rotation matrix: velodyne \Rightarrow camera
- $t_{velo}^{cam} \in R^{1 \times 3}$ is the translation vector: velodyne \Rightarrow camera

These two matrices are provided with the KITTI dataset. Using the transformation matrix in Eq. (2), velodyne coordinates are calibrated with the reference camera. In this dataset, images have been captured only in the forward direction. So, only LIDAR data points with *positive* x values are projected to the RGB color image. The fusion of the data from these two sensors (velodyne and camera) gives us a more detailed representation of the vehicle environment that can better support visual reasoning tasks at higher levels (e.g., detection and recognition). Figure 3 shows the result of fusing the point cloud shown in Figure 1 with the RGB image of the same scenario shown in Figure 2.

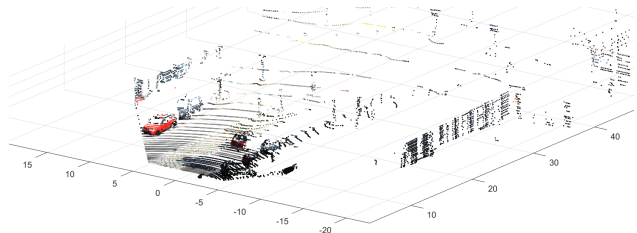


Figure 3: 6D model of the scenario shown in Figure 1

Vehicle Detection using PIHOG

The fusion of 3D point cloud data and RGB color image provides a six-dimensional map of the vehicle environment that is more versatile than individual representation. This 6D map can be utilized to support high-level visual inference (e.g., to understand the environment). As a part of understanding, the autonomous vehicle needs to detect both moving (e.g. other vehicles, motorcycles and pedestrians) and still (e.g. lane markers, traffic lights and signs etc.) objects on the road. In this work, we opt to focus on the detection of moving vehicles from the reconstructed map of the environment. For extracting features, position and intensity-included histogram of oriented gradient (PIHOG) [12] technique has been used, which is an extended version of regular

HOG [17] (a popular technique widely used in pedestrian detection algorithms). Because of the large and flat shape of the vehicle, some limitations of regular HOG feature descriptor may generate erroneous results. Two major drawbacks are summarized in [12] as follows

1. HOG is basically a histogram-based feature descriptor; no information about the location of the gradients is stored. Consequently, two completely different cells may have the same histogram as shown in Figure 4. Here, both cells have 16 pixels, and the gradient vector of each pixel has been illustrated using the red arrow. For simplicity, all gradients are assumed to have same magnitudes. Although, the two cells have different gradients, they have the same histogram of oriented gradients because both cells have the same number of 45° and 135° components.
2. Only edge information of an image is included in typical HOG features; intensity information is not preserved in HOG. Only edge-based features may not be sufficient to detect a vehicle.

Based on the above observations, one can observe that there remains opportunity for further improving the performance of HOG in vehicle detection technique by including image intensity and location of the gradients. Along this line of reasoning, Position and Intensity - included HOG (PIHOG or π HOG) has been introduced in [12] to detect vehicles in color/RGB images. In this paper, PIHOG has been exploited for vehicle detection from the 6D representation (XYZ+RGB) of the vehicle environment.

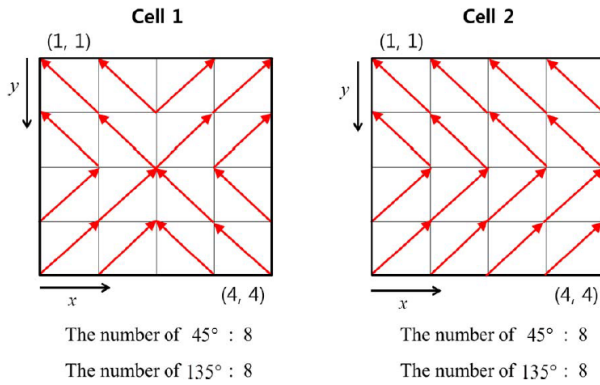


Figure 4: Two different cells with same histogram of gradients [12]

To facilitate the visual illustration of PIHOG's advantage, we project an example of the 6D map onto a 2D image. In this experiment, only the front view of the map has been used. This view can be generated by mapping the YZ plane to a 2D image, and using the RGB values from the 6D map (refer to Figure 5). It can be seen that the vehicles of interest are well distinguishable in this figure, which supports the goal of detecting the vehicles from this image (e.g., via SVM or deep learning techniques). The main advantage of this fused data over RGB image is to resolve the issue of *scale invariance*. In a regular RGB image, all the objects face the scaling effect - i.e. objects closer to the camera appear in larger shape; while the appearance of an object gets smaller as the camera distance increases. By contrast, as the 6D map gets the height information from the z-values of the point

cloud, objects from different distances appear to have the *same* heights in the projected images. In a nutshell, PIHOG is able to overcome the drawbacks of HOG-based approaches by including position and intensity features and achieving the desirable scale invariance. These two extra features will be elaborated in the next two subsections.



Figure 5: 2D front view of the 6D map shown in Figure 3

Position Features

Figure 4 illustrates that two cells with different gradient vectors can have same histogram (i.e. same HOG features). To make the features more distinguishable, the positions of oriented gradients are taken into consideration. Let $\theta(x, y, c)$ be the orientation of the gradient at (x, y) location of the c cell (given that $0 \leq \theta \leq 2\pi$). The orientations of the gradients are quantized in T bins and the expression of the orientation bin $B(x, y, c)$ is given by,

$$B(x, y, c) = \left\lceil \frac{T\theta(x, y, c)}{2\pi} \right\rceil, 0 \leq \theta \leq 2\pi, B(x, y, c) \in \{1, \dots, T\} \quad (3)$$

Then the means of x and y positions of the d^{th} bin has been calculated using the following expressions,

$$M_{x,d}^c = \frac{\sum_{x=1}^{c_x} \sum_{y=1}^{c_y} x \prod[B(x, y, c) = d]}{\sum_{x=1}^{c_x} \sum_{y=1}^{c_y} \prod[B(x, y, c) = d]} \quad (4)$$

and

$$M_{y,d}^c = \frac{\sum_{x=1}^{c_x} \sum_{y=1}^{c_y} y \prod[B(x, y, c) = d]}{\sum_{x=1}^{c_x} \sum_{y=1}^{c_y} \prod[B(x, y, c) = d]} \quad (5)$$

where, width and height of the c^{th} cell are represented as c_x and c_y respectively, $\prod(\cdot)$ is an indicator function that returns 1 if the argument is true, otherwise returns 0. Using equations 4 and 5, we have obtained two new features $P_c = [M_x^c, M_y^c]$ (where, $M_x^c = [M_{x,1}^c, \dots, M_{x,T}^c]$ and $M_y^c = [M_{y,1}^c, \dots, M_{y,T}^c]$) that include the position information of the gradients.

Intensity Features

To include the intensity information, intensity invariant region (IIR) based features have been extracted using all the positive (vehicle) images. Suppose, $V = \{s_1, s_2, \dots, s_{n_v}\}$ is the set of all positive vehicle images and $s_i = [s_{i,1}, s_{i,2}, \dots, s_{i,N}]^T$ is the i^{th} positive image; where, $s_{i,j}$ is the intensity of the j^{th} pixel in the i^{th} image. N is the total number pixels in each image, and n_v is the size of the set of positive images. In this experiment, all the sample images (both positive and negative) are resized to 48×48 images ($N = 2304$). As a first step of determining the IIR across the positive vehicle images, following equations are used to calculate the mean and standard deviation of the images,

$$M = \frac{1}{N_v} \sum_{i=1}^{N_v} s_i = [m_1, m_2, \dots, m_N]^T \quad (6)$$

$$\sigma = \sqrt{\frac{1}{N_v} \sum_{i=1}^{N_v} (s_i - M) \circ (s_i - M)} = [\sigma_1, \sigma_2, \dots, \sigma_N]^T \quad (7)$$

where, \circ denotes the component-wise multiplication. Figure 6 shows the mean image (a), and the standard deviation image (b) of the positive vehicle images.

The main idea of IIR is that, the regions where all the positive vehicle images have similar intensity values should have low standard deviations. That means, the intensity values in these regions are common for the vehicles regardless of their colors (these regions are defined as IIR) and can be used to distinguish between the vehicles and other objects on the roads. For the purpose of feature extraction, values of the standard deviation image are divided into K number of intervals. If the range of the values of k -th mask U_k is given by $[\epsilon_k, \epsilon_{k+1}]$, then the mask can be described by following equation,

$$U_k = \{j | \epsilon_k \leq \sigma_j \leq \epsilon_{k+1}, j = 1, 2, \dots, N\} \quad (8)$$

In the proposed method, 20 intervals (i.e. $K = 20$) have been used. As, low standard deviation values indicate the region of similar intensities for all the vehicles, only first five masks ($n = 5$) have been considered for feature matrix generation. Now, for a test image s , standard normal deviate image is computed as,

$$z = \left(\frac{1}{\sigma}\right) \circ (s - M) \quad (9)$$

Applying the first n IIR masks ($U_1, U_2, \dots, U_n; n = 5$) on z , the features correspond to the IIR masks can be computed by,

$$h_k = \frac{1}{|U_k|} \sum_{j \in U_k} z_j \quad (10)$$

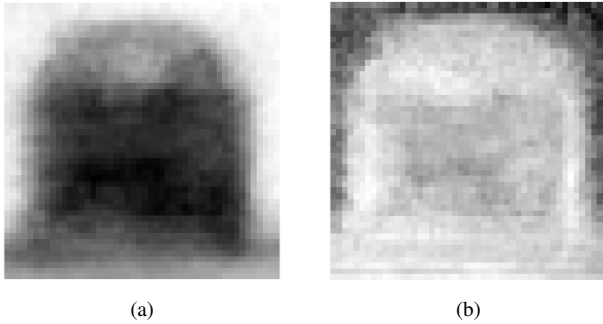


Figure 6: (a) Mean, and (b) standard deviation of all positive vehicle images

PIHOG Feature Formation and Vehicle Detection

Except the position and intensity features, PIHOG feature extraction follows the same procedure of the conventional HOG [17]. A sliding window (40×40 in this experiment) is used to divide the sample image into image blocks and all the blocks are reshaped to size 48×48 . Each block is decomposed into C number of cells ($C = 4$), and HOG features are extracted from each cell. The gradients in a cell are assigned to T bins ($T = 9$), i.e. dimension of extracted HOG features from each window is CT . The position feature (P_c) size for each cell is a $2T$ dimensional vector (T values in both x and y directions). Hence, a window

with C cells has position features of $2CT$ dimensions. The intensity features extracted from a window consists of n dimensional IIR feature vector h_k (where, $k = 1, 2, \dots, n$). So, the total length of the feature matrix is $3CT + n$. After combining all the features, complete feature matrix of PIHOG extracted from a window is defined as,

$$F_{PIHOG} = [F_{HOG}, P_1, P_2, \dots, P_c, h_1, \dots, h_n] \quad (11)$$

where, F_{HOG} represents the conventional HOG features, $[P_1, P_2, \dots, P_c]$ are the position features, and $[h_1, h_2, \dots, h_n]$ are intensity features. In this experiment, PIHOG features are extracted from both positive (vehicle) and negative (background, i.e. road surface, trees, buildings etc.) samples. In the training stage, a linear support vector machine (SVM) has been trained using the PIHOG feature extracted from the positive and negative samples. This trained model is later used to detect vehicles from a 2D front view image of the reconstructed environment.

Experimental Results

In our experiment, we first fuse the camera and LIDAR data to create a 6D representation to support the task of vehicle detection. Then we extract position and intensity-included HOG (PIHOG) features from the 2D projection (front view) of 6D representation (XYZ+RGB) of the vehicle environment. The extracted features are then used to train a SVM with linear kernel and the trained model is exploited to detect vehicles from the surrounding environment. The main advantage of this approach over using regular RGB image (from camera) is that it can resolve the scaling problem of moving objects in continuous video frames. As mentioned before, our approach preserves the actual Z-values of the points; therefore objects will appear of the same heights (independent of the distances from the sensor) in the projected images. This experiment has been conducted in five different scenarios (raw data - city and road environments) from the KITTI dataset [16]. For the training purpose, we have used 48×48 images of vehicles (positive) and background (negative) objects manually cropped from the 2D projection (front view) of 6D environment maps. A total of 215 images (102 positive, 113 negative) have been used in training phase. PIHOG has been applied to these positive and negative images for extracting features and a linear support vector machine (SVM) has been trained using these features. For testing purpose, a total of 125 frames are taken from the five scenarios (25 frames from each scenario). The size of the sliding window is 40×40 (with 50% overlapping), and each window is reshaped to the size of 48×48 before extracting PIHOG features. Some results of this experiment have been illustrated in Figure 7. Detected vehicles are highlighted in red boxes. The complete experimental results on test data are shown in Table 1, where both overall and frame-wise vehicle detection results are recorded. Ground truths have been set by manually labeling the actual location of the vehicles. The number of successful and wrong detection has been recorded for each frame. Detection accuracy is shown in percentage, and the wrong detection is expressed in objects per frame. Here, we can see that the overall accuracy is around 73%. Although it can be considered as pretty good, there is still room for further improvement. For instance, we have only used the front view of the map in this experiment, which can miss some vehicle because of occlusion. It is possible

to generate projected image of the 6D map from other perspectives, which can resolve the occlusion and further improve the detection accuracy.

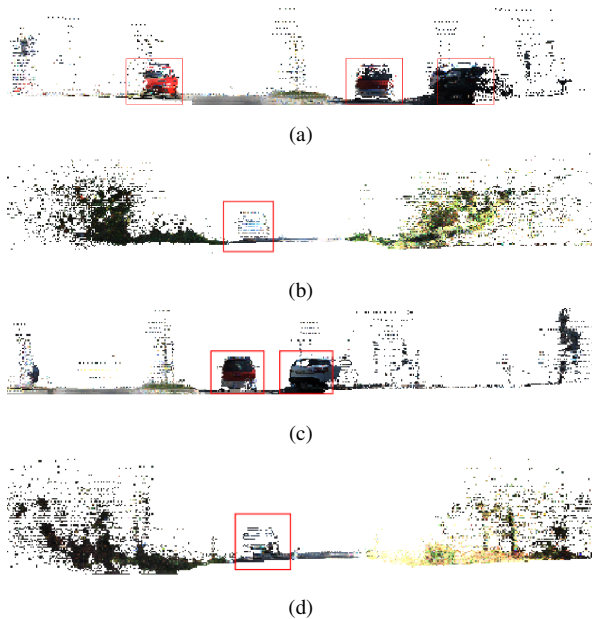


Figure 7: Results of PIHOG-SVM based vehicle detection

Table 1: Overall and frame-wise vehicle detection accuracy

Sequence	No. of Frames	No. of Vehicles (GT)	Accuracy (%)	Wrongly Detected (objects/frame)
1	25	109	66.06	0.04
2	25	26	76.92	0.04
3	25	30	83.33	0
4	25	26	80.77	0.8
5	25	60	76.67	0.4
Total	125	251	73.31	0.256

Conclusion

In this paper, a fusion technique has been proposed to detect vehicles to support autonomous vehicle applications. The proposed technique uses both camera image and LIDAR point cloud data to reconstruct a six dimensional map of the surrounding environment. A modified version of HOG (PIHOG) has been applied to this reconstructed map to extract scale-invariant features and train a linear SVM. This trained SVM model has been exploited to detect vehicles from the neighboring environment and achieved promising preliminary results.

References

[1] D. Geronimo, A. M. Lopez, A. D. Sappa and T. Graf, Survey of Pedestrian Detection for Advanced Driver Assistance Systems, *IEEE Transactions on Pattern Analysis and Machine Intelligence*, vol. 32, no. 7, pp. 1239 - 1258, 2010.

[2] L.-W. Tsai, J.-W. Hsieh and K.-C. Fan, Vehicle Detection Using Nor-

malized Color and Edge Map, *IEEE Transactions on Image Processing*, vol. 16, no. 3, pp. 850 - 864, 2007.

[3] D. Guo, T. Fraichard, M. Xie and C. Laugier, Color modeling by spherical influence field in sensing driving environment, in *Proceedings of the IEEE Intelligent Vehicles Symposium*, Dearborn, MI, USA, 2000.

[4] M. Bertozzi and A. Broggi, Vision-based vehicle guidance, *Computer*, vol. 30, no. 7, pp. 49-55, 1997.

[5] B. Vlž, H. Mielenz, R. Siegwart and J. Nieto, Predicting pedestrian crossing using Quantile Regression forests, in *2016 IEEE Intelligent Vehicles Symposium (IV)*, Gothenburg, Sweden, 2016.

[6] Navarro-Serment, L. E., C. Mertz and M. Hebert, Pedestrian detection and tracking using three-dimensional lidar data, *The International Journal of Robotics Research*, vol. 29, no. 12, pp. 1516-1528, 2010.

[7] C. Fernandez, D. F. Llorca, C. Stiller and M. A. Sotelo, Curvature-based curb detection method in urban environments using stereo and laser, in *2015 IEEE Intelligent Vehicles Symposium (IV)*, Seoul, South Korea, 2015.

[8] C. Premebida, J. Carreira, J. Batista and U. Nunes, Pedestrian detection combining RGB and dense LIDAR data, in *2014 IEEE/RSJ International Conference on Intelligent Robots and Systems*, Chicago, IL, USA, 2014.

[9] F. Zhang, D. Clarke and A. Knoll, Vehicle detection based on LiDAR and camera fusion, in *17th International IEEE Conference on Intelligent Transportation Systems (ITSC)*, Qingdao, China, 2014.

[10] A. C. Sidiya, A. H. M. Rubaiyat, Y. Fallah, G. Bansal, T. Shimizu and X. Li, Robust vehicle environment reconstruction from point clouds for irregularity detection, *2017 IEEE Intelligent Vehicles Symposium (IV)*, Los Angeles, CA, 2017, pp. 1085-1092.

[11] S. Sivaraman and M. M. Trivedi, Looking at Vehicles on the Road: A Survey of Vision-Based Vehicle Detection, Tracking, and Behavior Analysis, *IEEE Transactions on Intelligent Transportation Systems*, vol. 14, no. 4, pp. 1773 - 1795, 2013.

[12] J. Kim, J. Baek and E. Kim, A Novel On-Road Vehicle Detection Method Using π HOG, *IEEE Transactions on Intelligent Transportation Systems*, vol. 16, no. 6, pp. 3414 - 3429, 2015.

[13] F. Erbs, A. Barth and U. Franke, Moving vehicle detection by optimal segmentation of the Dynamic Stixel World, in *2011 IEEE Intelligent Vehicles Symposium (IV)*, Baden-Baden, Germany, 2011.

[14] B. Li, T. Zhang and T. Xia, Vehicle Detection from 3D Lidar Using Fully Convolutional Network, *arXiv preprint arXiv:1608.07916*, 2016.

[15] J. Eum, M. Bae, J. Jeon, H. Lee, S. Oh and M. Lee, Vehicle detection from airborne LiDAR point clouds based on a decision tree algorithm with horizontal and vertical features, *Remote Sensing Letters*, vol. 8, no. 5, pp. 409-418, 2017.

[16] A. Geiger, P. Lenz, C. Stiller and R. Urtasun, Vision meets robotics: The KITTI dataset, *International Journal of Robotics Research*, vol. 32, no. 11, pp. 1231-1237, 2013.

[17] N. Dalal and B. Triggs, Histograms of Oriented Gradients for Human Detection, in *IEEE Computer Society Conference on Computer Vision and Pattern Recognition (CVPR 2005)*, San Diego, CA, 2005.

[18] C. Cortes and V. Vapnik, Support-Vector Networks, *Machine Learning*, vol. 20, no. 3, pp. 273 - 297, 1995.

[19] Herrera, Daniel, Juho Kannala, and Janne Heikkil. "Accurate and practical calibration of a depth and color camera pair." *International Conference on Computer analysis of images and patterns*. Springer, Berlin, Heidelberg, 2011.

Author Biography

Abu Hasnat Mohammad Rubaiyat received his MS degree in Electrical Engineering from West Virginia University in 2017. He worked on reconstruction and understanding of neighboring environment of an autonomous vehicle using data from local sensors. He did his undergrad at Bangladesh University of Engineering and Technology in 2013, and then worked in SAMSUNG R&D Institute (Dhaka, Bangladesh) as Software Engineer till 2015 before starting his MS studies. Currently, he is doing his PhD in University of Virginia.

Yaser P. Fallah received his PhD from University of British Columbia, Canada, in 2007. He is currently an associate professor of Electrical and Computer Engineering at University of Central Florida. From 2011 to 2016, he was an assistant professor at West Virginia University. Prior to joining WVU, he worked as a research scientist at the University of California Berkeley, Institute of Transportation Studies (2008-2011). Dr. Fallah is an editor of IEEE Trans. on Vehicular Technology.

Xin Li received the B.S. degree with highest honors in electronic engineering and information science from University of Science and Technology of China, Hefei, in 1996, and the Ph.D. degree in electrical engineering from Princeton University, Princeton, NJ, in 2000. He was a Member of Technical Staff with Sharp Laboratories of America, Camas, WA from Aug. 2000 to Dec. 2002. Since Jan. 2003, he has been a faculty member in Lane Department of Computer Science and Electrical Engineering. His research interests include image/video processing, computer vision, biometrics and information security. Prof. Xin Li is an Fellow of IEEE.

Gaurav Bansal is a Principal Researcher at the Toyota InfoTechnology Center in Mountain View, CA, where he leads several research initiatives on the design of communication systems for Automated Driving. Gaurav represents Toyota in the Automakers' Vehicle Safety Communication Consortium and in the SAE, ETSI standardization bodies. Gaurav holds Electrical Engineering degrees from Indian Institute of Technology, Kanpur and The University of British Columbia.



Free access to this paper is brought to you with the generous support of ON Semiconductor.

All research funding for this paper is referenced in the text; unless noted therein, no research funding was provided by ON.